Article

Inspection of the Duality of a Verdazyl-Based Radical in Transition Metal Complexes: A #* Donor Ligand and a Magnetic Partner

Jean-Baptiste Rota, Lucie Norel, Cyrille Train, Nadia Ben Amor, Daniel Maynau, and Vincent Robert

J. Am. Chem. Soc., **2008**, 130 (31), 10380-10385 • DOI: 10.1021/ja802027u • Publication Date (Web): 09 July 2008

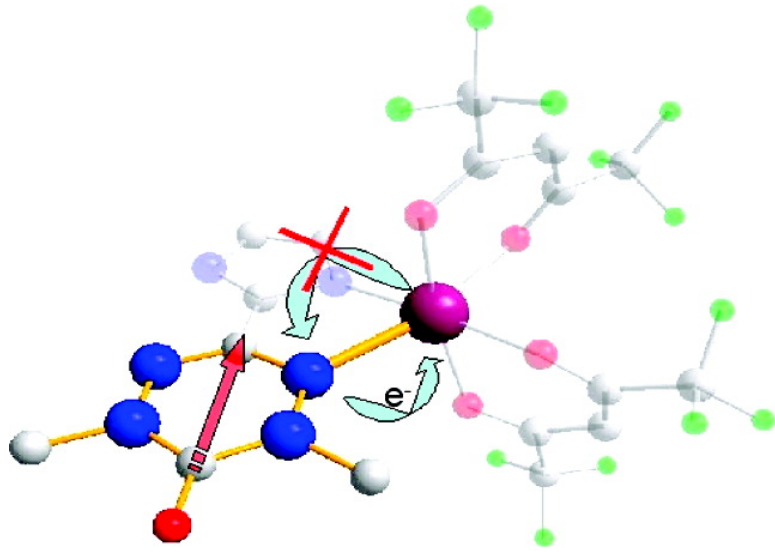

More About This Article

Additional resources and features associated with this article are available within the HTML version:

- Supporting Information
- Access to high resolution figures
- Links to articles and content related to this article
- Copyright permission to reproduce figures and/or text from this article

View the Full Text HTML

J|A|C|S
ARTICLES

Published on Web 07/09/2008

Inspection of the Duality of a Verdazyl-Based Radical in Transition Metal Complexes: A π^* Donor Ligand and a Magnetic Partner

Jean-Baptiste Rota,[†] Lucie Norel,[‡] Cyrille Train,[‡] Nadia Ben Amor,[§] Daniel Maynau,[§] and Vincent Robert*,[†]

Laboratoire de Chimie, Ecole Normale Supérieure de Lyon, 46 Allée d'Italie 69364 Lyon Cedex 07; Chimie Inorganique et Matériaux Moléculaires, UMR CNRS 7071, IFR 2769, UPMC Univ Paris 06, 4 place Jussieu, case 42, F-75005 Paris, France, and Laboratoire de Chimie et Physique Quantiques, 118 Route de Narbonne, 31062 Toulouse Cedex 04

Received May 28, 2008; E-mail: vincent.robert@ens-lyon.fr

Abstract: The behavior of a verdazyl-based radical bound to open-shell transition metal ions in the structurally and magnetically characterized [M(hfac)$_2$imvd°] (M = Mn, Ni; hfac = (1,1,1,5,5,5)hexafluoroacetylacetonate; imvd° = 3-(2′-imidazolyl)-1,5-dimethyl-6-oxoverdazyl) complexes is rationalized using ab initio wave-function-based calculations analysis. The calculated exchange coupling constants J ($H = -Js_M.s_{imvd°}$; $J_{Mn}^{calcd} = -63$ cm^{-1}, $J_{Ni}^{calcd} = 205$ cm^{-1}) are in excellent agreement with the experimental ones ($J_{Mn}^{exp} = -63$ cm^{-1}, $J_{Ni}^{exp} = 193$ cm^{-1}). Even though both rings are involved through the binding mode of the imvd° radical, the spin density remains essentially localized on the nitrogen-rich ring. The singularity stems from its bidentate coordinating character. The analysis of the correlated wave function suggests that the verdazyl-based radical acts as a π^* donor ligand which allows ligand-to-metal charge transfer and excludes metal-to-ligand charge transfer. This reflects the weak covalent character of the M-imvd° π coordination bond. From a magnetic point of view, the through-space exchange governs the ferromagnetic character in the Ni derivative up to 153 cm^{-1} as expected from a description limited to the magnetic orbitals. Nevertheless, the CI expansion displays the participation of excited doublet and quartet states (spin polarization) on the verdazyl moiety which leads to a significant additional ferromagnetic contribution (52 cm^{-1}). In the [Mn(hfac)$_2$imvd°] analogue, the antiferromagnetic contribution arising from kinetic exchange is only one-third of the observed exchange coupling constant. It is necessary to introduce dynamical correlation effects to quantitatively recover the exchange interaction in this compound. Since the π^* donor and spin-polarized characters of the verdazyl moiety dominate over the negligible polarizability of the imidazole part, it is concluded that the noninnocent nature of the imvd° radical is held by the verdazyl ring part.

1. Introduction

The synthesis and characterization of molecule-based magnetic systems have attracted considerable interest since spectacular properties can be anticipated[1–4] and evidenced in molecular magnetic clusters[5] and extended networks.[6–9] The featuring characteristics of such systems is the exchange coupling constant J. The sign and amplitude of the latter summarize the interactions between a limited number of localized electrons. Interestingly, the properties of the systems are mainly governed by these unpaired electrons and can be described by a Heisenberg−Dirac−Van−Vleck spin-only phenomenological Hamiltonian $H = -Js_1.s_2$ (HDVV). As a result of the spatially and energetically localized characters of the so-called magnetic orbitals,[10] the coupling constants and microscopic behavior are generally dominated by the nearest neighbors, possibly second-nearest neighbors,[11] interactions.

While the exchange constant values are experimentally accessible from temperature-dependent magnetic susceptibility measurements, large configurations interaction (CI) ab initio

[†] Ecole Normale Supérieure de Lyon.
[‡] UMR CNRS 7071.
[§] Laboratoire de Chimie et Physique Quantiques.

(1) Calzado, C. J.; Sanz, J. F.; Malrieu, J.-P. *J. Chem. Phys.* **2003**, *117*, 5158–5167.
(2) Suaud, N.; Lepetit, M.-B. *Phys. Rev. B* **2000**, *62*, 402–409.
(3) Sadoc, A.; de Graaf, C.; Broer, R. *Phys. Rev. B* **2007**, *75*, 165116.
(4) Borbas, E.; Caballol, R.; de Graaf, C.; Malrieu, J.-P. *Chem. Phys.* **2005**, *309*, 259–269.
(5) Gatteschi, D.; Sessoli, R. *Angew. Chem., Int. Ed.* **2003**, *42*, 268–297.
(6) Verdaguer, M.; Bleuzen, A.; Marvaud, V.; Vaissermann, J.; Seuleiman, M.; Desplanches, C.; Scuiller, A.; Train, C.; Garde, R.; Gelly, G.; Lomenech, C.; Rosenman, I.; Veillet, P.; Cartier et, F.; Villain, C. *Coord. Chem. Rev.* **1999**, *190−192*, 1023–1047.
(7) Maspoch, D.; Ruiz-Molina, D.; Veciana, J. *Chem Soc. Rev.* **2007**, *36*, 770–818.
(8) Fegy, K.; Luneau, D.; Ohm, T.; Paulsen, C.; Rey, P. *Angew. Chem., Int. Ed.* **1998**, *37*, 1270–1273.
(9) Clément, R.; Decurtins, S.; Gruselle, M.; Train, C. *Monatsh. Chem.* **2003**, *134*, 117–135.
(10) Kahn O. *Molecular Magnetism;* VCH: New York, 1993.
(11) Li, L.; Liao, D.; Jiang, Z.; Mouesca, J.-M.; Rey, P. *Inorg. Chem.* **2006**, *45*, 7665–7670.

10.1021/ja802027u CCC: $40.75

calculations[12,13] or density functional theory (DFT) broken symmetry approaches[14] have been successfully called for to elucidate the underlying mechanisms. The mapping of the eigenstates of the exact Hamiltonian into a HDVV model Hamiltonian relies on the definition of a model space consisting mainly of the neutral valence bond forms. Nevertheless, charge transfers between the magnetic partners are known to play a dominant role in the hierarchization of the spin states. The accurate evaluation of energy splittings of a few tens of wavenumbers and the identification of the microscopic phenomena are challenging issues for theoreticians. Even though DFT methods are remarkably adapted for large systems,[15] they may suffer from the nonunique definition of the exchange-correlation ingredient. Based on the difference dedicated configuration interaction (DDCI) wave function method,[16] impressive agreement with experimental values has been reported in various dinuclear[17] and trinuclear[18] magnetically coupled architectures. Nevertheless, these methods, which may take advantage of the local character of the interactions, are rather demanding since the wave function is expanded over large CI spaces.

Among the abundant class of multicentric architectures involving open-shell metal ions, systems based on paramagnetic ligands have turned out to be promising targets to enhance the exchange interactions.[19,20] In this respect, verdazyl radical (vd°) containing ligands represent an interesting route toward strongly coupled discrete[21–24] and extended[21,25] molecule-based magnetic systems. In particular, reactions with $M(hfac)_2 \cdot 2H_2O$ afforded the preparations of [$M(hfac)_2$(pyvd°)] (M = Ni, Mn, and pyvd° = 3-(2′-pyridyl)-1,5-dimethyl-6-oxoverdazyl)[21] and [$M(hfac)_2$(imvd°)] (imvd° = 3-(2′-imidazolyl)-1,5-dimethyl-6-oxoverdazyl)[24] series of complexes. Their magnetic behaviors have been analyzed using a metal ion−radical interaction picture.[24] The nature and amplitude of the intramolecular interactions are sensitive to the metal ion and verdazyl radical partner since strong ferromagnetic ($J_{Ni\text{-}pyvd°} = 240$ and $J_{Ni\text{-}imvd°} = 193$ cm^{-1}) and antiferromagnetic ($J_{Mn\text{-}pyvd°} = -45$ and $J_{Mn\text{-}imvd°} = -63$ cm^{-1}) behaviors were reported. The analysis based on a crystal field picture and symmetry considerations has provided a rational, though qualitative, interpretation of the spectacular magnetic behavior of these compounds. The impressively high $|J|$ values and the difference between imvd°- and pyvd°-based complexes suggest that several efficient mechanisms must be involved in magnetic exchange couplings. Nevertheless, no theoretical inspection, which may clarify the role of the apparently noninnocent radical as a ligand, has been reported so far.

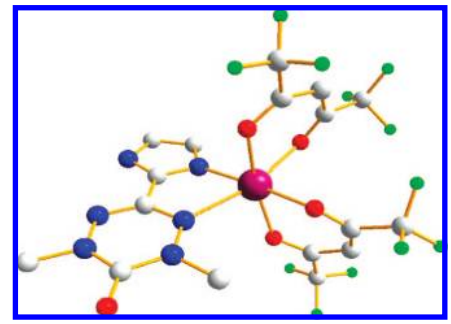

Figure 1. Structure of the [$M(hfac)_2$imvd°] (M = Ni, Mn) complexes. H atoms were omitted for clarity.[24]

How much does the electronic configuration of the metal ion and the ligand field produced by the verdazyl containing ligand itself control the exchange interaction is questionable. Part of the answer is to be found in the academic picture, which analyzes the through-bond and through-space mechanisms between two spin carriers. Starting from the radical localization on the oxoverdazyl part,[23] several mechanisms can be anticipated. Direct exchange, which favors the high-spin (HS) over the low-spin (LS) states,[26] is undoubtedly effective from the spatial proximity of the magnetic partners. In contrast, kinetic exchange which introduces electron hoppings, namely ligand-to-metal and metal-to-ligand charge transfers (LMCT and MLCT), stabilizes the LS state. Such CT can be favored through a polarization of the vd° and M ion environments as reported in the literature.[27] The exchange coupling may proceed through different channels in a superexchange picture. Not only is the σ vd°−M bond likely to contribute but correlations effects involving the pyridine or imidazole coordinating part may also play a role. Finally, the radical being simultaneously a bidentate ligand and a magnetic partner, the participation of the local excited spin states on the vd° moiety should be examined.

Thus, to allow further rationalization in the design of synthetic targets involving the promising class of verdazyl-based ligands, we felt that a theoretical inspection might be desirable to elucidate the magnetic behavior of model complexes where interactions are limited to two spin carriers. CI calculations were performed on the imvd° radical and [$M(hfac)_2$imvd°] (M = Mn, Ni) complexes (Figure 1) using the crystal structure of these compounds[24] in order to (i) identify the magnetic orbitals and relevant states of the ligands, (ii) evaluate the different contributions to the exchange interaction, and (iii) rationalize the behaviors of the imvd° ligand ($s = {}^1/_2$) when bound to Ni^{2+} high-spin (hs, $s = 1$) and Mn^{2+} high-spin (ls, $s = 5/2$) cations.[26]

(12) (a) Calzado, J. C.; Cabrero, J.; Malrieu, J. P.; Caballol, R. *J. Chem. Phys.* **2002**, *116*, 2728–2747. (b) Calzado, J. C.; Cabrero, J.; Malrieu, J. P.; Caballol, R. *J. Chem. Phys.* **2002**, *116*, 3985–4000.
(13) Neese, F. *J. Chem. Phys.* **2003**, *119*, 9428–9443.
(14) Noodlemann, L.; Norman, J. G. *J. Chem. Phys.* **1979**, *70*, 4903–4906.
(15) (a) Rodriguez-Fortea, A.; Ruiz, E.; Alvarez, S.; Alemany, P. *Dalton Trans.* **2005**, 2624–2629. (b) Moreira, I. P. R.; Costa, R.; Filatov, M.; Illas, F. *J. Chem. Theory Comput.* **2007**, *3*, 764–774. (c) *Principles and Applications of Density Functional Theory in Inorganic Chemistry II*; Ruiz, E., Kaltsoyannis, N., McGrady, J. E., Eds.; Springer-Verlag: New York, 2004; Vol. 113, pp 71−102.
(16) Miralles, J.; Castell, O.; Caballol, R.; Malrieu, J.-P. *Chem. Phys.* **1993**, *172*, 33–43.
(17) Cabrero, J.; de Graaf, C.; Bordas, E.; Caballol, R.; Malrieu, J.-P. *Chem.−Eur. J.* **2003**, *9*, 2307–2315.
(18) Le Guennic, B.; Petit, S.; Pilet, G.; Chastanet, G.; Luneau, D.; Ben Amor, N.; Robert, V. *Inorg. Chem.* **2008**, *46*, 572–577.
(19) (a) Herebian, D.; Wieghardt, K.; Neese, F. *J. Am. Chem. Soc.* **2003**, *125*, 10997–11005. (b) Messaoudi, S.; Robert, V.; Guihéry, N.; Maynau, D. *Inorg. Chem.* **2006**, *45*, 3212–3216. (c) Luneau, D.; Rey, P. *Coord. Chem. Rev.* **2005**, *249*, 2591–2611.
(20) Koivisto, B. D.; Hicks, R. G. *Coord. Chem. Rev.* **2005**, *249*, 2615–2630.
(21) Brook, D. J.; Lynch, V.; Conklin, B.; Fox, M. A. *J. Am. Chem. Soc.* **1997**, *119*, 5155–5162.
(22) Hicks, R. G.; Lemaire, M. T.; Thompson, L. K.; Barclay, T. M. *J. Am. Chem. Soc.* **2000**, *122*, 8077–8078.
(23) Jornet, J.; Deumal, M.; Ribas-Arino, J.; Beapark, M. J.; Robb, M. A.; Hicks, R. G.; Novoa, J. *Chem.−Eur. J.* **2006**, *12*, 3995–4005.
(24) Norel, L. Pointillard, F.; Train, C.; Chamoreau, L.-M.; Boubekeur, K.; Journaux, Y.; Brieger, A.; Brook, D. J. R. *Inorg. Chem.* **2008**, *47*, 2396–2403.
(25) Pointillart, F.; Train, C.; Herson, P.; Marrot, J.; Verdaguer, M. *New J. Chem.* **2007**, *31*, 1001–1006.
(26) Lower cases will be used throughout the text to describe the magnetic state of the magnetic partners while upper cases will refer to the total spin states of the complexes.
(27) De Loth, P.; Cassoux, P.; Daudey, J.-P.; Malrieu, J.-P. *J. Am. Chem. Soc.* **1981**, *103*, 4007–4016.

Wave functions calculations were favored since they allow us to quantitatively distinguish the different underlying mechanisms contributing to the exchange coupling between the 3d metal ion and the organic radical ligand. From the duality of the imvd° (i.e., spin carrier and ligand), the polarization of the verdazyl π electronic system is analyzed in analogy with open-shell metal ion behaviors which may contribute to exchange coupling through Hund and non-Hund forms.[28] By introducing the dynamical correlation effects, the breathings of the environments upon charge fluctuations are then considered to discriminate between LMCT and MLCT. Finally, the noninnocence of the magnetic ligand is reconsidered in the light of our detailed inspection.

2. Computational Details

The coupling between magnetic moments localized on the metal ion and radical gives rise to two magnetic states, HS and LS,[26] while the energy difference $\Delta E = E_{LS} - E_{HS}$ is related to the exchange interaction J defined in the HDVV Hamiltonian ($\Delta E_{Mn} = E(S = 2) - E(S = 3) = 3J_{Mn}$ and $\Delta E_{Ni} = E(S = {}^1/_2) - E(S = {}^3/_2) = {}^3/_2 J_{Ni}$). The microscopic origin of the exchange interaction can be investigated by means of quantum theoretical calculations. With this goal in mind, the difference dedicated configuration interactions (DDCI) method has been designed and applied to evaluate vertical energy differences.[16] To reduce the computational cost, simplified structures for [M(hfac)$_2$imvd°] compounds were constructed by replacing the CF_3 groups by H atoms on the reported crystallographic data.[24] The importance of trifluoro methyl substituents has been analyzed previously.[29] First, complete active-space self-consistent field (CASSCF) calculations are performed to generate a reference space including the leading electronic configurations in the desired spin multiplicities. The complete active spaces (CAS) include the unpaired electrons on the different partners (i.e., metal ion and imvd° radical) and the corresponding molecular orbitals (MOs). For the imvd° ligand, the CAS was enlarged to look for other spin states which might compete with the expected $s = {}^1/_2$ ground-state doublet. All CASSCF calculations were performed using the Molcas 6.0 package[30] and available ANO-type functions. Ni and Mn atoms were described with a (9s6p5d2f)/[6s5p3d1f] contraction. A (9s6p5d)/[3s2p1d] contraction was used for the first coordination sphere N and O atoms. In order to treat all the imvd° radical atoms on the same footing, a similar extended basis set (9s6p5d)/[3s2p1d] was used whereas a smaller [3s2p] basis set was chosen for the carbon atoms of the hfac ligands. Finally, the H atoms were depicted with a minimal basis set (3s)/[1s].

The dynamical polarization and correlation effects were then incorporated using the DDCI method as implemented in the CASDI code.[31] It has been clearly demonstrated that a bare valence-only description is not relevant to grasp such energy differences.[12] Thus, one should include selected configurations reached by excitations on top of the CASSCF wave function. As the number of degrees of freedom (i.e., holes in doubly occupied (inactive) MOs or particules generated in empty (virtual) MOs) grows, the successive DDCI-1, DDCI-2, and DDCI-3 levels are reached by expanding the CI space. DDCI-1 corresponds to CAS + single excitations (1-hole 1-particle determinants are included and lead to a CI space which grows as $N_o \times N_v$, N_o and N_v being the number of occupied and virtual MOs). In the DDCI-2 space, determinants corresponding to double excitations from the occupied to the active MOs (2-hole determinants, i.e. ${N_o}^2 + {N_v}^2$ more determinants), and from the active to the virtual MOs (2-particle determinants) are added. Finally, DDCI-3 includes 1-hole, 2-particle and 2-hole, 1-particle determinants, and a significant CI space enlargement results (${N_o}^2 \times N_v\, N_o \times {N_v}^2$ more determinants). This demanding procedure incorporates all configurations that are known from second-order perturbation analysis to be necessary to reach spectroscopic accuracy.[27] Since the DDCI philosophy relies on the simultaneous characterization of different states which share similar spatial descriptions, one has to initially determine a set of common MOs to build up the CI space. For both systems, the CASSCF ground-state MOs were used, that is, quintet ($S = 2$) and quartet ($S = {}^3/_2$) for the Mn and Ni compounds, respectively. Nevertheless, the size of the complexes and the need for extended basis sets on the radical ligand are incompatible with a full DDCI-3 calculation. Thus, two different strategies were used to reach this demanding, though necessary, description of correlation effects. In a first approach, DDCI-1 calculations were performed on both states ($S = 2$, 3 and $S = {}^1/_2$, ${}^3/_2$ for Mn and Ni compounds, respectively[26]), and the corresponding density matrices were calculated. The difference between the two density matrices was then diagonalized. The resulting orbitals with occupation numbers close to zero are expected to play the same role in both states. Thus, they should not affect the energy difference and are discarded. The remaining ones are the so-called dedicated orbitals.[26] A DDCI-3 calculation is then performed using this truncated basis set. A second original route is to select the most relevant determinants according to spatial proximity considerations. Using localized orbitals (LOs), a topological matrix is built, which indicates whether two LOs are effectively interacting (i.e., spatially close one to the other). The criterion used in this work to decide if LOs i and j are "spatially close" is the corresponding exchange integral K_{ij} which should be larger than a given threshold. The convergence of the energy differences with this threshold was checked down to the 0.003 au value. This strategy has been recently used to successfully investigate low-energy spectrum of large multicentric systems.[18,33] Let us mention that accurate wave-function-based calculations involving partly delocalized spin densities remain challenging in the microscopic understanding of magnetic interactions.

3. Results

As preliminary investigations, calculations were performed on the imvd° system to identify the low-energy spectrum of this magnetic partner. Thus, a CAS(15,12) was considered to include all the valence π electrons in the corresponding MOs. As reported in the pyvd° doublet ground state,[23] the unpaired electron is mainly localized on the verdazyl moiety (Figure 2).

Thus, as the system binds to the metal, one may expect the nature of the exchange interaction to be controlled by the electronic circulation between the π_2* (SOMO) and some symmetry-adapted metal-centered d-type MOs. The first excited quartet state $s = {}^3/_2$ lies 2.7 eV higher in energy, and results from a triplet $\pi_1 \rightarrow \pi_3$* excitation on the $s = {}^1/_2$ picture (Figure 2).[26] The appearance of this $(\pi_1)^1(\pi_2^*)^1(\pi_3^*)^1$ electronic configuration is strongly suggestive of the participation of 3-electron Heisenberg-like states, namely a quartet (Hund state) and two doublets. The respective roles of these Heisenberg states (i.e., single occupations of π_1, π_2*, and π_3* MOs) on the ligand cannot be excluded to fully understand the physicochemical properties of the complexes. As seen in Figure 2, the π_1 and π_3* valence MOs display non-negligible contributions on the imidazole moiety. How efficient are the metal−ligand electron

(28) (a) Bastardis, R.; Guihéry, N.; De Graaf, N. *Phys. Rev. B* **2007**, *76*, 132412. (b) Guihéry, N. *Theor. Chem. Acc.* **2006**, *116*, 576–586.
(29) Carvajal, M. A.; Aronica, C.; Luneau, D.; Robert, V. *Eur. J. Inorg. Chem.* **2007**, *46*, 4434–4437.
(30) Karlström, G.; Lindh, R.; Malmqvist, P-A.; Roos, B. O.; Ryde, U.; Veryazov, V.; Widmark, P-O.; Cossi, M.; Schimmelpfennig, B.; Neogrady, P.; Seijo, L. *Comput. Mater. Sci.* **2003**, *28*, 222–239.
(31) Ben Amor, N.; Maynau, D. *Chem. Phys. Lett.* **1998**, *286*, 211–220.
(32) Miralles, J.; Caballol, R.; Malrieu, J.-P. *Chem. Phys.* **1991**, *153*, 25–37.
(33) Bories, B.; Maynau, D.; Bonnet, M.-L. *J. Comput. Chem.* **2007**, *28*, 632–643.

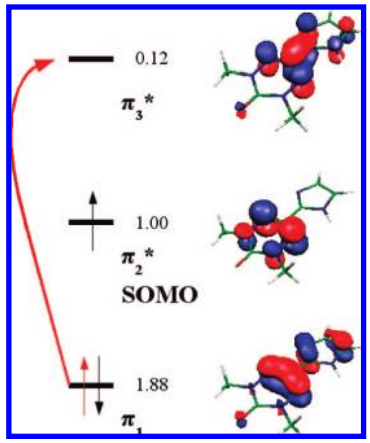

Figure 2. Valence MOs of the imvd° radical. The arrow indicates the $\pi_1 \rightarrow \pi_3^*$ excitations giving rise to the Heisenberg states, a quartet $s = {}^3/_2$ and two doublets $s = {}^1/_2$ built on the valence MOs.[26] Occupation numbers in the doublet ground state $(\pi_1)^2(\pi_2^*)^1$ are given.

Table 1. Energy Difference (cm^{-1}) between $S = {}^1/_2$ and $S = {}^3/_2$ States and J_{Ni}^{calcd} Values in the Ni Derivative[26]

Ni	ΔE_{Ni}	J_{Ni}^{calcd}
CASSCF	229	153
DDCI-1	261	173
DDCI-2	260	173
DDCI-3[a]	332	221
DDCI-3[b]	308	205

[a] Dedicated MO. [b] Localized MO.

Table 2. Energy Difference (cm^{-1}) between $S = 2$ and $S = 3$ states and J_{Mn}^{calcd} Values in the Mn Derivative[26]

Mn	ΔE_{Mn}	J_{Mn}^{calcd}
CASSCF	−70	−23
DDCI-1	−202	−67
DDCI-2	−190	−63

transfers and the participation of the Heisenberg-like states are parts of the issues which can be extracted from ab initio calculations. Let us stress that the same picture should hold for the pyvd° radical which behaves similarly when bound to Ni^{2+} and Mn^{2+} open-shell ions. However, the lack of crystal structure precluded the theoretical inspection of [M(hfac)$_2$pyvd°] complexes.

On the basis of the imvd° low-energy spectrum, we performed large CI calculations to investigate and analyze the behaviors of [Ni(hfac)$_2$(imvd°)] and [Mn(hfac)$_2$(imvd°)] complexes. By allowing the occupations of 3 electrons in 3 MOs (e_g* and π_2* (SOMO) for the Ni^{2+} ion and imvd°, respectively) for the Ni derivative and six electrons in six MOs ($t_{2\ g}$, e_g* and π_2* (SOMO) for the Mn^{2+} ion and imvd°, respectively) for the Mn analogue, CASSCF calculations were first carried out to analyze the low-energy parts of the spectra. These active spaces (valence-only description) allow one to account at zeroth order for all the leading "neutral" (i.e., M^{2+}-imvd°) and charge transfer configurations (i.e., M^{+}-imvd^{+} and M^{3+}-imvd^{-}). As seen in Tables 1 and 2, the CASSCF spin gaps read $\Delta E_{Mn} = -70\ cm^{-1}$ and $\Delta E_{Ni} = 229\ cm^{-1}$. The CASSCF ground-state active MOs of both systems correspond to the singly occupied metal d-type MOs and the imvd° π_2* (SOMO) (Figure 3).

Let us stress that the MOs of the LS and HS states are very similar, as expected from the spatial localization of the electrons in magnetic systems. Thus, it is possible to use the same MOs to calculate the energies of the ground and the excited states.

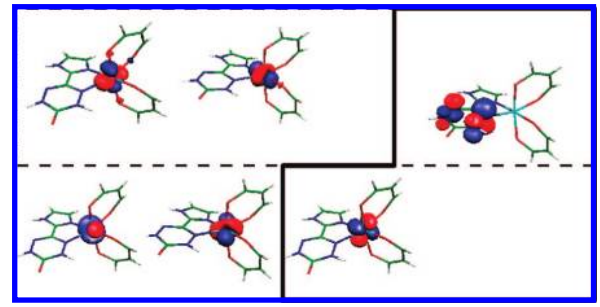

Figure 3. Active MOs in the Mn complex. Overlapping orbitals (full line) and Ni complex active MOs (dotted line) are highlighted.

Quantitatively, the energy difference based on the ground-state MOs accounts for ∼95% of the CASSCF energy differences ΔE_{Ni} and ΔE_{Mn}. While a qualitative description falls in these preliminary valence-only calculations, a quantitative picture calls for the subsequent CI expansion. As a matter of fact, the calculated CASSCF J values exhibit noticeable difference with the experimental ones. This is a clear indication that other mechanisms must be considered to fully understand the exchange interaction between the two magnetic partners. They are highlighted using a DDCI treatment on the basis of the ground states MOs.

As seen in Tables 1 and 2, the exchange interactions in the [Ni(hfac)$_2$(imvd°)] and [Mn(hfac)$_2$(imvd°)] complexes are significantly influenced by the correlations effects introduced by the DDCI treatment. They indeed modify the exchange interactions by several tens of wavenumbers as compared to the CASSCF values. The remarkable agreement of the calculated values ($J_{Ni}^{calcd} = 205\ cm^{-1}$, $J_{Mn}^{calcd} = -63\ cm^{-1}$) with the experimental ones[24] ($J_{Ni}^{exp} = 193\ cm^{-1}$, $J_{Mn}^{exp} = -63\ cm^{-1}$) demonstrate the ability of this original localization technique to treat rather extended magnetic systems. Moreover, the step-by-step introduction of supplementary interactions offers a deeper understanding of the multiple contributions to the exchange interaction through the inspection of the wave functions at each level of calculation. Any mechanism which stabilizes the LS state should introduce electron circulation between the metal ion and the radical ligand in a kinetic exchange picture. In the Ni derivative, the ligand-to-metal charge transfer is forbidden for symmetry reasons[22] since the singly occupied MOs of the Ni^{2+} ion are orthogonal to the verdazyl π_2* (SOMO). One may wonder whether back-donation (i.e., metal-to-ligand charge transfer) would contribute to the exchange interaction. Indeed, a back-donation would decrease the spin density on the verdazyl ligand and consequently reduce the J value. A natural candidate for such intramolecular electron transfer would be the essentially doubly occupied symmetry-adapted d_{xy} orbital. However, the analysis of the DDCI-3 wave function shows that the participation of such mechanism is completely negligible. On the contrary, spin polarization effects—which are introduced at the DDCI-1 level—stabilize the HS state by ∼30 cm^{-1}. Interestingly, the DDCI-3 treatment brings another ∼40 cm^{-1} to the energy splitting and reaches spectroscopy accuracy. The size-consistency error was taken into account using the Davidson's correction on the DDCI-3 results and leads to a rather small change (5 cm^{-1}) in the energy differences.

These results are to be contrasted to the ones obtained for the Mn analogue. Even though the electrostatics is the same (divalent metal ions), the electronic configuration and spin state of Mn^{2+} are likely to modify the possible LMCT and MLCT.

Table 3. Relative Weights of the Quartet $s = {}^3/_2$ and Doublet $s = {}^1/_2$ Spin States in the HS and LS States in the [Ni(hfac)$_2$imvd°] Compound as a Function of the Level of Calculation

ligand spin state	$s = {}^3/_2$	$s = {}^1/_2$
DDCI-1	0.97	1.09
DDCI-3	1.49	1.45

Our DDCI-1 calculations (see Table 2) are in very good agreement with experimental values. The demanding DDCI-3 calculations were performed by expanding the CI space constructed on localized orbitals. Extrapolation leads to a satisfactory $J_{Mn} = -53$ cm^{-1} value. However, the need for a large active space to depict the $s = {}^5/_2$ Mn^{2+} ion precluded any fully quantitative DDCI-3 calculations. The extracted exchange value can only be considered as an evaluation, still in fairly good agreement. The symmetry-adapted d_{xy} orbital is singly occupied for manganese(II). Thus, an effective LMCT Mn^+-imvd$^+$ tends to stabilize the LS quintet state. This is the well-known kinetic exchange contribution attributed to the overlap of the verdazyl π_2* (SOMO) and Mn d_{xy} orbital (Figure 3). DDCI-1 calculations take into account the stabilization of this LMCT through dynamical spin polarization. The electrostatic response of the environments to the charge fluctuations between the two spin carriers is responsible for a ~130 cm^{-1} antiferromagnetic contribution (see CASSCF and DDCI-1 results in Table 2). Interestingly, the MLCT involving the singly occupied Mn-d_{xy} orbital is completely negligible, as observed in the Ni derivative. The reluctance to back-donation seems to be of particular importance in the control of magnetic properties.

4. Discussion

The comparison between the two complexes is rather insightful into the possibility to generate organic radicals, which may exhibit both ligand and magnetic characters. Noninnocent ligands have been much studied in the literature considering their impressive ability to undergo multistep redox reactions.[34–36] This class of ligands can be selectively oxidized and reduced, leaving the formal oxidation state of the metal unchanged. Such behavior suggests that intramolecular electron transfers between the ligand and the metal are likely to occur. Similar observations possibly accompanied by spin state changes have led to the "excited state coordination chemistry"[19] and "valence tautomerism"[34] concepts. Thus, there is strong experimental and theoretical evidence to consider the metal ions and bound open-shell ligands on the same footing. Starting from the traditional picture, which couples two magnetic centers through a bridging moiety, a valence-only picture is very insightful into the qualitative understanding of the magnetic interactions. Nevertheless, significant variations in the coupling constants values have been observed in the verdazyl-based complexes.[20]

Regarding the [Ni(hfac)$_2$imvd°] derivative, the wave functions analysis (see Table 3) shows that two mechanisms lead to strong ferromagnetism, namely (i) the reluctance to back-donation (MLCT) that concentrates spin density on the verdazyl moiety of the imvd° ligand, and (ii) a spin polarization effect involving triplet and singlet $\pi_1 \rightarrow \pi_3$* excitations on the verdazyl moiety (Figure 2). These excitations localized on the verdazyl moiety give rise to local $s = {}^3/_2$ and $s = {}^1/_2$ spin states on the ligand.

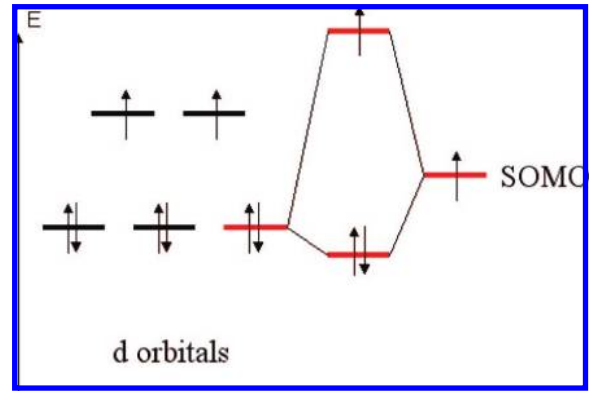

Figure 4. Unfavorable 3 electron−2 orbital interaction in the Ni compound.

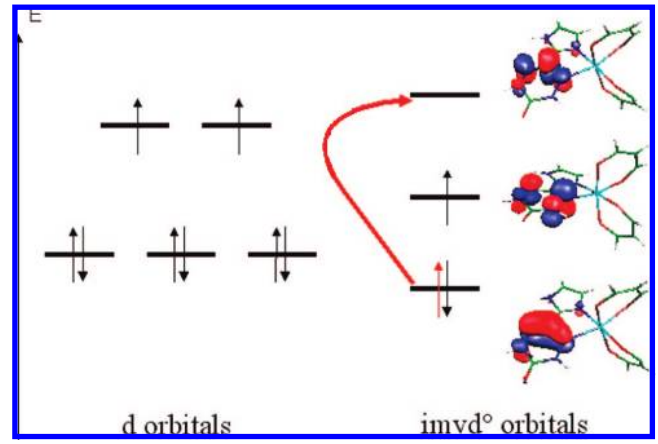

Figure 5. Spin polarization mechanism in the Ni compound, leading in particular to a quartet character on the imvd° radical.

The negligible back-donation phenomenon can be understood from a 3 electron−2 orbital interaction monoelectronic picture, which is not likely to offer any stabilization (Figure 4). To rationalize this observation, the energy of the MLCT state was calculated ~6 eV above the Ni complex quartet ground state. Such delocalization is not favored since it formally increases the occupation of the antibonding MO π_2*. As a consequence, the ligand remains open-shell when coordinated to the Ni^{2+} ion.

In contrast, spin polarization turns out to be the leading mechanism beyond the valence-only description (Figure 5). This mechanism is known to effectively participate in the HS−LS hierachization when ligand orbitals are involved.[12,29]

The singularity of the radical, being both a spin carrier and a ligand, is demonstrated by its rather important contribution to the exchange interaction. When necessary (and possible) DDCI-3 calculations are performed, the enhancement of the ferromagnetic character can be understood from the HS and LS wave functions reading.[26] The ground-state HS wave function displays a non-negligible $(\pi_1)^1(\pi_2^*)^1(\pi_3^*)^1$ electronic configuration which splits into 80% and 20% Heisenberg-type doublet and quartet characters, respectively. As seen in Table 3, the amplitudes of the $\pi_1 \rightarrow \pi_3$* quartet ($s = {}^3/_2$) and doublet ($s =$

(34) (a) Gütlich, P.; Dei, A. *Angew. Chem., Int. Ed. Engl.* **1997**, *36*, 2734–2736. (b) Dei, A.; Gatteschi, D.; Sangregorio, C.; Sorace, L. *Acc. Chem. Res.* **2004**, *37*, 827–835.
(35) (a) Evangelio, E.; Ruiz-Molina, D. *Eur. J. Inorg. Chem.* **2005**, *15*, 2957–2971. (b) Bin-Salomon, S.; Beber, S.; Franzen, S.; Feldheim, D. L.; Lappi, S.; Schultz, D. A. *J. Am. Chem. Soc.* **2005**, *127*, 5328–5329.
(36) (a) Spikes, G. H.; Bill, E.; Weyhermuller, T.; Wieghardt, K. *Angew. Chem., Int. Ed.* **2008**, *47*, 2973–2977. (b) Lu, C. C.; Bill, E.; Weyhermuller, T.; Bothe, E.; Wieghardt, K. *J. Am. Chem. Soc.* **2008**, *130*, 3181–3197.

$^1/_2$) excitations in the two states are very similar in weight, as expected if the imvd° ligand were isolated. The relative importance of these mechanisms is greatly enhanced as one goes from DDCI-1 to DDCI-3 calculations, the weights of the $\pi_1 \rightarrow \pi_3^*$ quartet ($s = {}^3/_2$) and doublet ($s = {}^1/_2$) in the LS state being reduced by 1.49 and 1.45, respectively, as compared to their values in the HS state. Thus, this variation can be attributed to both magnetic partner and ligand natures of the imvd° radical. This radical exhibits configurations with single occupations of the π_1, π_2^*, and π_3^* orbitals (so-called Heisenberg-type states) whose contributions are modulated as binding occurs. The $\pi_1 \rightarrow \pi_3^*$ polarization effects account for more than 25% of the exchange interaction. Interestingly, the participation of the $s = {}^3/_2$ quartet Hund state on the ligand[26] has a strong analogy with the reported importance of non-Hund forms on magnetically coupled metal ions systems.[28] Finally, the orbitals involved in this excitation are more localized on the verdazyl part than they were on the isolated ligand (Figure 2 and 5). To which extent these MOs tend to get more relocalized might be an explanation for the difference between the imvd° or pyvd° compounds.

For both Ni and Mn complexes, one may then wonder how much the polarizability of the environments (i.e., hfac ligands) and the spectator electrons (i.e., σ M-imvd° bond) are likely to modify the HS−LS[26] splitting. The systems at hand feature interaction between magnetic orbitals of different nature (mostly atomic-like on the metal ion, delocalized on the imvd°), which may differently respond to dynamical charge fluctuations (MLCT and LMCT). In particular, the imvd° radical is rather puzzling since the metal-to-ligand intramolecular electron transfer generating a M^{3+}-imvvd$^-$ configuration is not observed in the wave function. Conversely, the Mn^+-imvvd$^+$ LMCT in the Mn compound is significantly enhanced through the dynamical polarization of the hfac ligands. Its relative variation weight in the wave function between CASSCF and DDCI-1 levels is more than 15%. Quantitatively, the polarizability of the Mn^{2+} environment is tremendously important since it conveys 65% of the antiferromagnetic character. The net result is an π^* ligand-to-metal donation, resulting in a weak covalent character of the Mn−ligand bond. Besides, the imidazole part which can be seen as the radical environment turns out to be innocent in the magnetic exchange mechanism (Figure 6).

The duality of the imvd° radical being simultaneously a ligand and a magnetic partner supports the strong analogy with noninnocent ligands. Nevertheless, in contrast with noninnocent ligands where all the atoms of the chelating ring play a significant role in the exchange interaction,[19] the participation of the imidazole part in the magnetic exchange processes is almost negligible. The spin polarization mechanisms of the radical (Heisenberg-like character) are essentially localized on the verdazyl moiety. The ligand behavior arises from the antibonding character of the verdazyl moiety-centered π_2^* (SOMO) which discriminates between the LMCT and MLCT.

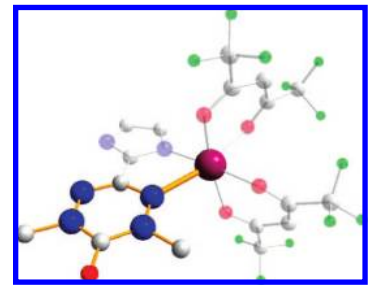

Figure 6. The magnetic exchange interaction is solely due to the verdazyl moiety of the bidente imvd° ligand.

5. Conclusion

Wave-function-based calculations were performed to understand the magnetic behavior of the imvd° radical in [Ni(hfac)$_2$imvd°] and [Mn(hfac)$_2$imvd°], which can be considered as model compounds for this type of verdazyl radical complexes containing open-shell transition metal ions. Even though a qualitative description is accessible through a valence-only picture, large CI calculations led to very good agreement with experimental data and, hence, to a rationalization of the strong exchange coupling interactions origin in these model complexes. The featuring mechanisms, which account for a significant part of the magnetic behavior can be attributed to the verdazyl moiety of the ligand. From the wave function analysis, the antibonding π^* character of the SOMO favors LMCT, whereas the MLCT channel is excluded and the verdazyl moiety remains essentially doublet character. Nevertheless, spin polarization effects (i.e., Heisenberg-like quartet and doublet characters of imvd°) have been identified and account for an important ferromagnetic contribution. In contrast to noninnocent ligands, which can undergo intramolecular redox reactions, the imidazole moiety does not participate in the exchange coupling mechanisms through CT transfer. The provided detailed inspection using wave function calculations clarifies and quantifies the mechanisms at work in [M(hfac)$_2$imvd°] model complexes: the verdazyl-based radical behaves as a π^* donor ligand and a magnetic partner, whereas the redox-innocent imidazole moiety is likely to modulate the total exchange interaction. This analysis is an important step in the rational design of synthetic targets involving members of the promising class of verdazyl-based ligands.

Acknowledgment. The authors thank CNRS, UPMC−Univ Paris 06, DFG (SPP 1137) and ANR "fdp Magnets" Project for financial support.

JA802027U